Microchim Acta (2017) 184:2081–2088
DOI 10.1007/s00604-017-2210-7

ORIGINAL PAPER

Voltammetric dopamine sensor based on a gold electrode modified with reduced graphene oxide and Mn_3O_4 on gold nanoparticles

Zufu Yao [1] · **Xin Yang** [2] · **Youya Niu** [3] · **Feng Wu** [2] · **Yangjian Hu** [2] · **Yaqi Yang** [2]

Received: 18 October 2016 / Accepted: 20 March 2017 / Published online: 1 April 2017

Abstract The authors describe an amperometric sensor for dopamine (DA) which has a working potential as low as +0.02 V (vs. SCE). It makes use of a nanocomposite consisting of reduced graphene oxide (rGO) and manganic manganous oxide (Mn_3O_4) in a film of Nafion on gold nanoparticles deposited on a gold electrode. The composite was characterized by X-ray powder diffractometry (XRD), Fourier transform infrared spectroscopy (FTIR) and field emission scanning electron microscopy (FE-SEM). The electrochemical properties of the modified electrode were investigated by cyclic voltammetry, electrochemical impedance spectroscopy (EIS) and amperometric methods. After method optimization, the amperogram displays a linear range extending from 1.0 $\mu mol\cdot L^{-1}$ to 1.45 $mmol\cdot L^{-1}$ with a limit of detection as low as 0.25 $\mu mol\cdot L^{-1}$ (at an S/N ratio of 3). The modified electrode was employed for the determination of DA in injection solution samples with satisfactory results.

Keywords Nanocomposite · Nafion film · Electrochemical sensor · XRD · FTIR · FE-SEM · Cyclic voltammetry · EIS · Amperogram

Introduction

Dopamine (DA) is involved in the hormonal, renal, cardiovascular and central nervous systems. Therefore, sensitive determination of DA is important for the evaluation of therapeutic efficacy and molecular disease diagnosis [1, 2]. Many techniques and approaches have been established for the detection of DA, such as the electrochemical technique (ET) [3–5], electrochemiluminescence [6], chromatography [7, 8] and fluorometry [9, 10]. Among these methods, ET is considered to be an ideal choice due to its high sensitivity, ease of operation, low cost, fast response and in situ detection. Since DA is an easily oxidized compound, ET based on its anodic oxidation has been reported for quantitative determination [11, 12]. Unfortunately, DA detection usually involves interference from some co-existing species including ascorbic acid (AA). AA can also be oxidized easily on the working electrode. Moreover, the oxidation of the mixture of AA and DA often appears as an overlapping voltammetric response on the unmodified electrode and is difficult to distinguish [13]. Hence, the selective determination of DA is a challenge for researchers [14, 15].

To improve measurement sensitivity and selectivity for DA determination, one effective approach is to choose sensitive and selective materials to sensitize the electrode. Jin [16] reported on the use of a $Cu_2O@Pt/C$ composite modified electrode which they used to eliminate interference by AA and uric acid (UA) in the determination of DA. The Co_3O_4 nanograin-decorated reduced graphene oxide (rGO) composite modified glassy carbon electrode (GCE) was developed by

Electronic supplementary material The online version of this article (doi:10.1007/s00604-017-2210-7) contains supplementary material, which is available to authorized users.

✉ Xin Yang
01yangxin@163.com

[1] Hunan Provincal Key Laboratory for Ethnic Dong Medicine Research, Hunan University of Medicine, Huaihua 418000, People's Republic of China

[2] Key Laboratory of Rare Earth Optoelectronic Materials & Devices, College of Chemistry and Materials Engineering, Huaihua University, Huaihua 418000, People's Republic of China

[3] Department of Medical Cell Biology & Genetics, Hunan University of Medicine, Huaihua 418000, People's Republic of China

Numan for the sensitive and selective determination of DA [17]. An electrochemical sensor for detecting DA was fabricated by Ejaz [18], using 1,4-bis (aminomethyl) benzene and $Co(OH)_2$ at the graphene oxide (GO) surface. Sivasubramanian [19] introduced an electrochemical sensor using Cu_2O decorated rGO composite for the selective detection of DA. Khudaish [20] described a novel surface material consisting of poly(2,4,6- triaminopyrmidine) decorated with gold nanoparticles (Au) on a GCE based on electrochemical polymerization. Although the aforementioned materials have excellent performance and signals, there is still a need for a novel composite which exhibits higher selectivity and sensitivity for the determination of DA.

Reduced graphene oxide (rGO) is a widely-used graphene nanomaterial. Recently, rGO-based materials have emerged as a novel nanomaterial for the fabrication of DA electrochemical sensors [21–23]. As a member of the transition metal oxide family, the uses of manganic manganous oxide (Mn_3O_4) have been explored in several fields including energy storage [24], supercapacitors [25], lithium-ion batteries [26] and electrochemical sensors [27]. As far as we know, an electrode modified with Mn_3O_4 has not been reported for the electroanalysis of DA. Various supports assembled with Au as modified electrodes have been selected as promising candidates for the electroanalysis of DA [28–30]. Nafion solution was widely employed to disperse various nanomaterials. The interference from AA during DA determination can partly be avoided by modifying the electrode surface with Nafion film. However, the use of Nafion film alone cannot solve the sensitivity problem [31]. Modifying the nanomaterials onto the electrode surface is one of the effective ways to improve sensitivity. Given these facts, we expect that rGO and Mn_3O_4, in combination with Au composite and the Nafion film, will have promising electrochemical activities for the electrochemical detection of DA.

An electrochemical sensor based on rGO-Mn_3O_4/Nafion film supporting different sized particles of Au on a modified gold electrode (GE) is reported and used for the amperometric analysis of DA with high selectivity and sensitivity at a working potential as low as +0.02 V (vs. SCE). Due to the low working potential, the modified electrode showed convincingly improved selectivity. Furthermore, the modified electrode possessed noticeably enhanced peak current and superior electrochemical activity for DA determination. Finally, it was employed to determine DA in injection solution samples with excellent recovery and accuracy.

Experimental

Chemicals and apparatus

$Mn(Ac)_2 \cdot 4H_2O$, graphite powder, nafion solution (5% (m:m)), chloroauric acid hydrate ($AuCl_3 \cdot HCl \cdot 4H_2O$, 99.99%) were purchased from Sinopharm Medicine Holding Co., Ltd. (http://www.sinoreagent.com/). Dopamine hydrochloride and ascorbic acid (AA) were obtained from Sigma (http://www.sigmaaldrich.com/). All chemicals used in the experiments were of analytical reagent grade. DA injection solution samples were purchased from Huaihua University (2016.6). The 0.1 $mol \cdot L^{-1}$ Na_2HPO_4 and NaH_2PO_4 stock solutions were mixed in different proportions to prepare phosphate buffer (PB) with various pH values. Doubly distilled water was used throughout (18.2 MΩ·cm resistance).

An X-ray powder diffractometer (XRD) was employed to study the crystallization degrees of the composite (Cu Kα radiation = 1.54056 nm, Ultima IV, Rigaku, http:// www.rigaku.com/en). The Fourier transform infrared spectroscopy (FTIR) of the composite were characterized with the KBr pellet (IR prestige-21, Shimadzu, http:// www.shimadzu.com.cn/). The surface morphologies of different electrodes were observed by means of field emission scanning electron microscopy (FE-SEM) (Sigma HD, Zeiss, http://www.zeiss.com.cn/corporate/zh_cn/home.html). All electrochemical measurements were carried out on an electrochemical workstation (CHI 660D, CH Instruments, http://www.chinstruments.com/), which was connected to the classical three electrode system. The saturated calomel electrode (SCE) was used as the reference electrode, the platinum wire was used as auxiliary electrode and the rGO-Mn_3O_4/Nafion-Au modified GE (Φ = 3 mm) was used as the working electrode.

Preparation of rGO-Mn_3O_4 composite

Graphene oxide (GO) was synthesized from natural graphite by the modified Hummers method [32]. 25.0 mg of GO was ultrasonicated in the mixed solvent of 50.0 mL absolute ethanol and H_2O (*v:v* = 9:1) for one hour to obtain a homogeneous suspension of 0.5 $mg \cdot mL^{-1}$ GO. Next, 0.005 mol of $Mn(AC)_2 \cdot 4H_2O$ was dissolved into the GO suspension under stirring. Subsequently, the mixed solution was sealed in a 100 mL Teflon-lined stainless steel autoclave. The temperature was raised to 200 °C and maintained for 12 h. Finally, the autoclave was cooled to room temperature. The precipitates were rinsed with water and absolute alcohol many times, followed by drying at 50 °C for 48 h. The product was labeled as rGO-Mn_3O_4 composite.

Fabrication of the modified electrode

To obtain a homogeneous suspension, 25.0 mg of rGO-Mn_3O_4 composite were dispersed into 50.0 mL of Nafion solution (0.5% (m:m)) under ultrasonication. The GE was polished with chamois leather containing 100 nm and 30 nm alumina slurry in succession, followed by ultrasonication treatment with HNO_3, absolute ethanol and doubly distilled water. 5.0 μL of rGO-

Mn_3O_4/Nafion dispersion was coated onto the GE's surface and kept at room temperature until dry (denoted as GE│rGO-Mn_3O_4/ Nafion). The modification of different sized particles of Au onto the surface of GE│rGO-Mn_3O_4/ Nafion electrode was obtained through the use of the simple electroless plating method described in our previous report [33]. Briefly, the GE│rGO-Mn_3O_4/Nafion electrode was immersed in 0.36 mol·L^{-1} ethylenediamine solution for 3.0 h at room temperature. Subsequently, it was inserted into 1.0 mmol·L^{-1} $AuCl_3·HCl·4H_2O$ solution for 2.5 h, Au^{3+} was bound to the surface of -NH_2 group. Different sizes of Au particle were obtained by reduction reactions of varying duration using 0.1 mol·L^{-1} $NaBH_4$ solution as the reducing agent. Finally, the modified electrode (denoted as GE│ rGO-Mn_3O_4/Nafion-Au) was rinsed with water and dried in an air atmosphere before use. The formation mechanism of rGO-Mn_3O_4/Nafion film supporting different sized particles of Au is illustrated in Fig. 1. For comparison, the Nafion solution (0.5% (m:m)) was dropped on the GE to fabricate the GE│Nafion electrode.

Results and discussion

Choice of materials

Gold has a high density of available active sites as well as a large electrochemically active surface area for the electrochemical reaction of DA. This results in a high-performance amperometric response for DA molecule detection. The interference from AA when determining DA can partly be avoided by modifying the electrode surface with Nafion film. The rGO-Mn_3O_4/Nafion film supporting different sizes of Au particle can be achieved via a simple electroless plating method. The amperometric response to DA detection is greatly effected by the respective particles and synergistic effects of the composite. In addition, different sizes of Au loading on the rGO-Mn_3O_4/Nafion film also influence the amperometric response.

Characterization of the rGO-Mn_3O_4 composite

The crystalline structure of GO, rGO and rGO-Mn_3O_4 were characterized by XRD. The GO's XRD pattern shows one typical diffraction peak at 2θ = 10.6°. This indicates that the introduction of many epoxy, carbonyl, hydroxyl and carboxyl groups attached to the sides and edges of the graphite [32]. The diffraction peak at about 2θ = 23° of rGO is quite in accordance with that of graphite [33]. In Fig.S1, the peak at close to 23° can be indexed to the graphitic plane (002) of rGO. All other peaks of rGO-Mn_3O_4 composite are well-matched with Mn_3O_4 which are consistent with the JCPDS card (No. 24–0734) [25].

Stretches of alkoxy (1060 cm^{-1}), epoxy C-O (1230 cm^{-1}), carboxyl C-O (1410 cm^{-1}), aromatic C = C (1620 cm^{-1}), C = O (1730 cm^{-1}) and O-H (3400 cm^{-1}) can be found in the FTIR of GO, in good agreement with our previous report

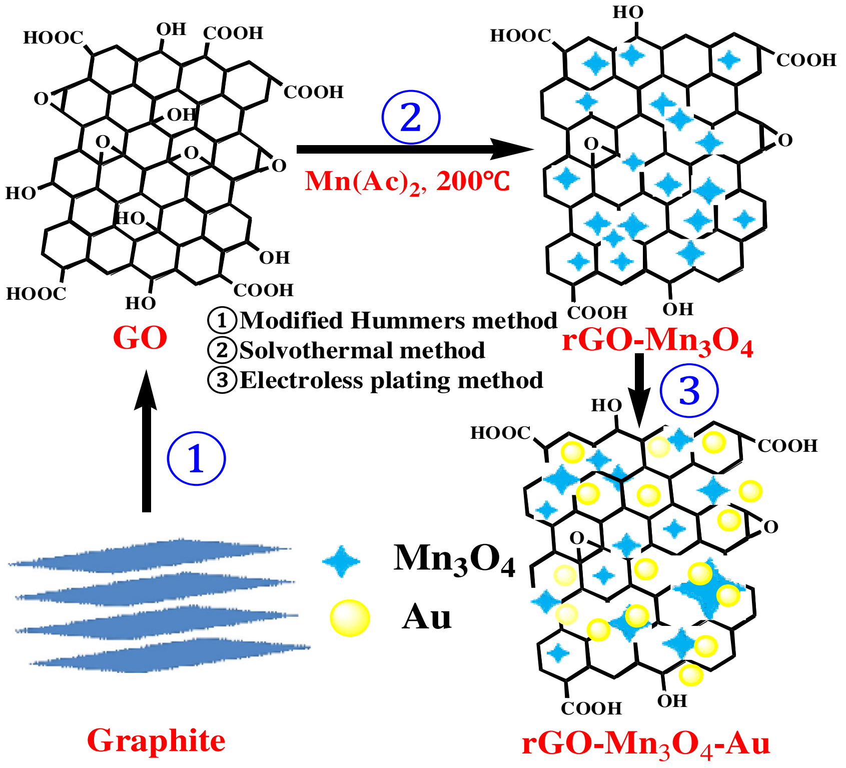

Fig. 1 Illustration of the formation of rGO-Mn_3O_4/Nafion film supported different sizes of Au

[33]. However, these peaks for oxygen-containing functional groups disappear or are weakened in the FTIR of both rGO and rGO-Mn_3O_4 composite. Moreover, three additional characteristic peaks can be found at 413, 515 and 618 cm^{-1}, which can be attributed to the band-stretching mode of the octahedral sites, the coupling mode between Mn-O octahedral sites and the stretching modes of tetrahedral sites, respectively (Fig.S2) [31]. The FTIR results also confirm the formation of rGO-Mn_3O_4 composite.

Characterization of the the surface morphologies of the different electrodes

Fig. 2-a presents the smooth surface morphology of the GE. Uniform Nafion film appears on the GE│Nafion electrode (Fig. 2-b). The surface of the GE│rGO-Mn_3O_4/Nafion electrode exhibits some thin wrinkles of rGO in the magnified SEM image and the Mn_3O_4 nanoparticles with a diameter of about 30 nm are well dispersed on the rGO (Fig. 2-c). Well-distributed Au with an average diameter of about 60 nm can also be found on the rGO-Mn_3O_4 composite after the electroless plating of Au onto the GE│rGO-Mn_3O_4/Nafion electrode (Fig. 2-d).

Electrochemical properties of different electrodes

The electrochemical properties of the different electrodes were evaluated by cyclic voltammetry (CV) in 0.1 mol·L^{-1} KCl solution containing 5.0 mmol·L^{-1} $K_3[Fe(CN)_6]$ as the redox probe. As depicted in Fig. S3, the current densities are found to be GE│rGO-Mn_3O_4/Nafion-Au (Fig. S3-d) > GE│rGO-Mn_3O_4/Nafion (Fig. S3-c) > GE (Fig. S3-a) > GE│Nafion (Fig. S3-b). The current density at the GE│Nafion is slightly lower than that at the GE, implying that Nafion reduces the redox current density. Compared with GE, a higher redox current density of the GE│rGO-Mn_3O_4/Nafion means an enhanced redox of the $[Fe(CN)_6]^{-3/-4}$ used as the probe, which can be ascribed to the large effective electroactive surface area of the rGO-Mn_3O_4 composite. Due to the large surface area as well as the unique electrochemical properties of Au, the redox current at the GE│rGO-Mn_3O_4/Nafion-Au electrode is higher than that at the GE│rGO-Mn_3O_4/Nafion electrode.

Electrochemical impedance spectroscopy (EIS) was used to evaluate the interfacial properties of the various electrodes. Nyquist plots for the four different electrodes are shown in Fig. S4. The higher frequency region with distinct semicircular corresponds to the electron transfer of the electrochemical reaction. The lower frequency region with the linear section corresponds to the diffusion limited process of the electrochemical reaction. A Randles circuit was employed to fit the EIS data (see inset in Fig. S4), including the double-layer capacitance (Q), Warburgh impedance (Zw), charge transfer resistance (Rct) and solution resistance (Rs). Rct is employed to describe the conduction capacity of the electrode indirectly, which is equal to the diameter of the semicircle. The Rct values of the GE (Fig. S4-a), GE│Nafion (Fig. S4-b), GE│rGO-Mn_3O_4/Nafion (Fig. S4-c) and GE│rGO-Mn_3O_4/Nafion-Au (Fig. S4-d) electrodes were calculated to be 120, 2980, 1450 and 780 Ω, respectively. Indicating that the conductivity of the GE│rGO-Mn_3O_4/Nafion-Au electrode is

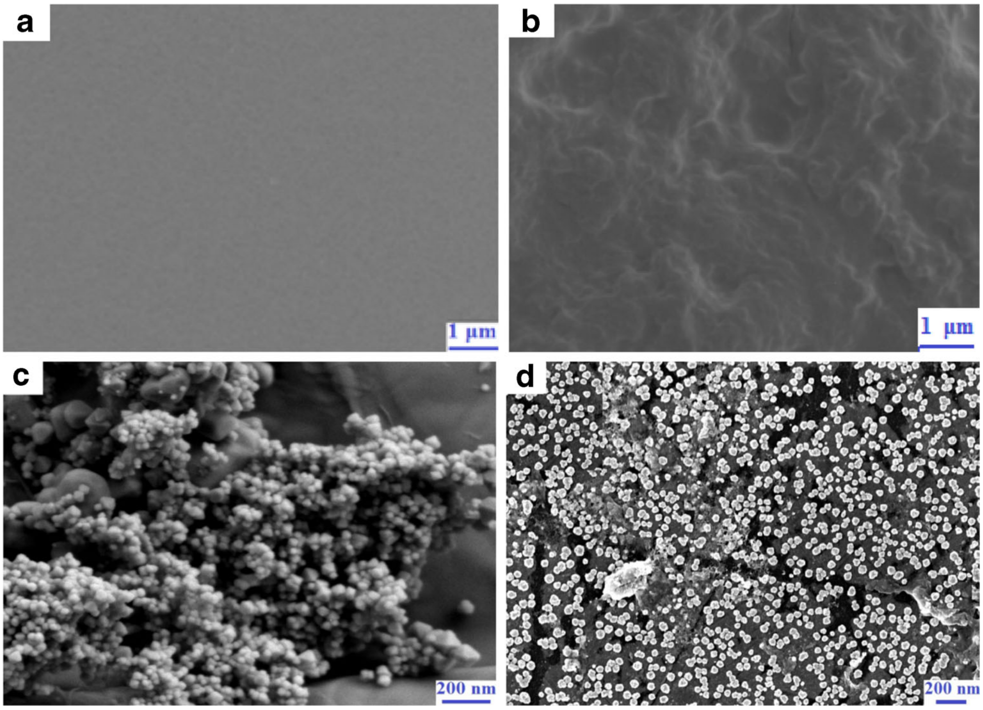

Fig. 2 FE-SEM images of the GE (**a**), GE│Nafion (**b**), GE│rGO-Mn_3O_4/Nafion (**c**) and GE│rGO-Mn_3O_4/Nafion-Au (**d**) electrodes

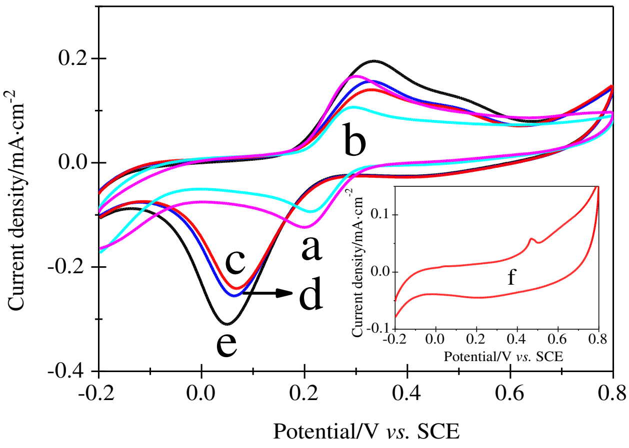

Fig. 3 CVs of the GE (**a**), GE│Nafion (**b**), GE│rGO-Mn_3O_4/Nafion (**c**) and GE│rGO-Mn_3O_4/ Nafion-Au (**d**) electrodes in 0.1 mol·L^{-1} PB containing 0.4 mmol·L^{-1} DA. (**d**) electrode in 0.1 mol·L^{-1} PB containing 0.6 mmol·L^{-1} DA (**e**) and 0 mmol·L^{-1} DA (**f**)

higher than that of both of the GE│rGO-Mn_3O_4/Nafion and GE│Nafion electrodes.

Electrochemical behaviors of DA at different electrodes

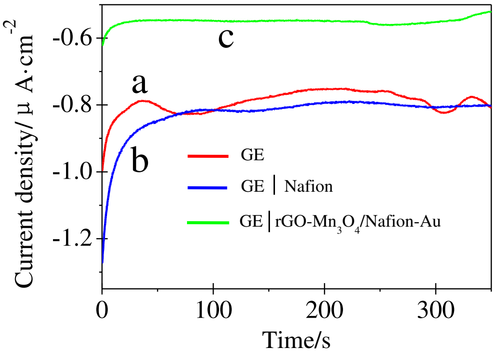

Fig. 5 i-t responses of the GE (**a**) and GE│Nafion (**b**) upon successive addition of various concentrations of DA from 1.0 µmol·L^{-1} to 1.0 mmol·L^{-1} and the GE│rGO-Mn_3O_4/Nafion-Au (**c**) electrode upon successive additions of various concentrations of AA from 1.0 µmol·L^{-1} to 1.0 mmol·L^{-1} at an applied potential of +0.02 V

Fig. 3 depicts the CV responses of different electrodes in PB. The CV measurements were recorded in pH = 4.5 PB at a scan rate of 0.1 v·s^{-1}. For 0.4 mmol·L^{-1} DA, a pair of redox peaks were found on the GE (Fig. 3-a). Owing to the insulativity of Nafion film, the GE│Nafion electrode showed a poor electrochemical response to DA (Fig. 3-b). For the GE│rGO-Mn_3O_4/Nafion electrode (Fig. 3-c), a cathodic peak for DA at +0.05 V was observed. The electron transfer is facilitated by the uniformly distributed rGO-Mn_3O_4 composite in the Nafion film. The rGO-Mn_3O_4 composite serves as the electron mediator. Compared with the GE and GE│Nafion, the reduction peak at GE│rGO-Mn_3O_4/Nafion shifted negatively. This implies that the rGO-Mn_3O_4 composite takes effect in the electro-reduction of DA. Moreover, the reduction peak potential of DA on the GE│rGO-Mn_3O_4/Nafion electrode, which can be as low as +0.05 V, is favorable for the electroanalysis of DA because interference from other electro-active species is reduced. There was an increase in overall voltammetric signal after the surface of the GE│rGO-Mn_3O_4/Nafion electrode was electroless plated with Au (Fig. 3-d). In addition, the reduction peak current at the GE│rGO-Mn_3O_4/Nafion-Au electrode increased with increasing DA concentration (Fig. 3-e), revealing the potential for the use of the GE│rGO-Mn_3O_4/ Nafion-Au electrode in DA determination. There was a depolarization of the GE│rGO- Mn_3O_4/Nafion-Au electrode in PB (Fig. 3-f).

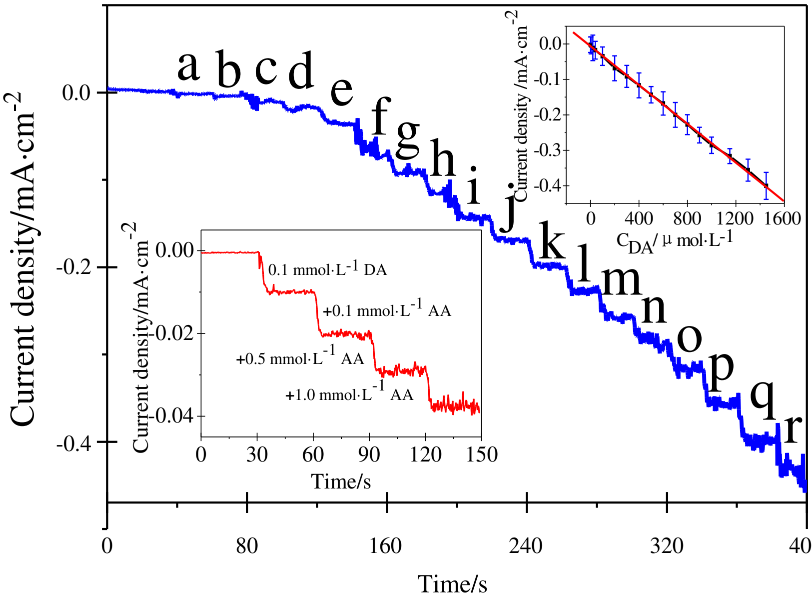

Fig. 4 The amperogram of the modified electrode upon successive addition of various concentrations of DA: (**a**) 1.0, (b) 4.0, (**c**) 15.0, (**d**) 20.0, (**e**) 60.0, (**f**)-(o)100.0, (p)-(r)150.0 µmol·L^{-1}. The insets display the current response upon successive additions of 0.1 mmol·L^{-1} DA with different concentrations of AA and the linear calibration curve

Table 1 Comparison of some other methodologies and different DA electrochemical sensors

Methodologies or Electrodes	Linear range/μmol·L^{-1}	LOD/μmol·L^{-1}	References
Electrochemiluminescence	0.005–500	0.0017	[6]
Chromatography	-	0.042	[7]
Fluorometry	0.0001–10	0.00002	[9]
GCE│GO-BAMB^{a}-Co(OH)$_2$	3–20, 25–100	0.4	[18]
GCE│MnOOH	1.2–200	0.1	[34]
GCE│F3GA^{b}-PDAN^{c}	5.0–100	0.1	[35]
GE│SWCNT^{d}/Fe$_2$O$_3$	3.2–31.8	0.36	[36]
GCE│er-GO-Ni	0.05–50	0.01 ± 0.00003	[37]
GCE│GO-MWCNT/MnO$_2$/Au	0.5–2500	0.17	[38]
GE│rGO-Mn$_3$O$_4$/Nafion-Au	1.0–1450	0.25	This work

- not provided. ^{a} 1,4-bis(aminomethyl)benzene. ^{b} Cibacron blue. ^{c} Poly-1,5-diaminonaphthalene. ^{d} Single-walled carbon nanotubes

The current is a reduction current and the operating potential corresponds to the reduction of the quinoid form of DA. DA in its native state (o-hydroquinone) cannot be reduced further at +0.05 V. Thus, Mn$_3$O$_4$ probably oxidizes DA to dopamine quinone which is then detected.

Optimization of experimental conditions

The following parameters were optimized: (a) volume of the casting solution. (b) concentration of the rGO-Mn$_3$O$_4$ composite in the casting solution. (c) supporting electrolyte and pH. (d) plating time. (e) electrochemical working potential. The respective data and figures are given in the Electronic Supporting Material (ESM). We found the following experimental conditions to give the best results: (a) a casting solution volume of 5.0 μL. (b) a concentration of rGO-Mn$_3$O$_4$ composite in the casting solution of 0.5 mg·mL^{-1}. (c) a 0.1 mol·L^{-1} PB at pH = 4.5. (d) a plating time of 200 s (Fig. S5). (e) an electrochemical working potential of +0.02 V (vs. SCE).

Amperometric responses of DA on the modified electrode

With all experimental conditions optimized, the amperogram of the response of the modified electrode to successive additions of DA at +0.02 V (vs. SCE) is shown in Fig. 4. With the addition of DA, the cathodic current increased rapidly and reached a steady state signal within 3 s, demonstrating the high sensitivity of the modified electrode. The insets in Fig. 4 show the response current at the modified electrode has a wide linear relationship to the concentration of DA in the range from 1.0 to 1450 μmol·L^{-1}. The equation for the regression line is I (mA·cm^{-2}) = −0.0062–2.7395 × 10^{-4} C_{DA} (C: μmol·L^{-1}) (R = 0.9995). A limit of detection (LOD) as low as 0.25 μmol·L^{-1} was achieved based on a signal to noise ratio (*S/N*) equal to 3.

The GE (Fig. 5-a) and GE│Nafion (Fig. 5-b) were subjected to similar experiments. There were no obvious response currents to DA in either case. The results suggest that rGO-Mn$_3$O$_4$ and Au really play an important role in enhancing the currents of DA on the electrode surface. AA is one of major interfering species affecting electrochemical DA detection in the analysis of real samples. The modified electrode showed no obvious response to AA (Fig. 5-c). The insets in Fig. 4 also show the amperometric response of the modified electrode to 0.1 mmol·L^{-1} determination DA with various concentrations of AA. The interferences observed from AA are negligible. In fact, the applied potential, which is as low as +0.02 V (vs. SCE) on the modified electrode, is immune to AA interference [13].

The DA electrochemical sensor presents comparable or even better analytical performances than many other methodologies or DA electrochemical sensors, as summarized in

Table 2 Determination of DA content in injection solution (n = 5, values are mean ± *RSD*, mmol·L^{-1})

Sample	Labeled value	This method	Added	Found	Recovery/%
1	52.7	52.5 ± 0.033	100.0	153.7 ± 0.021	101.2
2	52.7	53.4 ± 0.040	100.0	152.6 ± 0.038	99.2
3	52.7	52.4 ± 0.036	100.0	154.8 ± 0.043	102.4
4	52.7	52.6 ± 0.025	100.0	152.9 ± 0.019	100.3
5	52.7	52.7 ± 0.011	100.0	153.8 ± 0.035	101.1
6	52.7	52.7 ± 0.041	100.0	154.4 ± 0.023	101.7

Table 1. This can be explained by the high surface-to-volume ratio, excellent electrochemical activity, and synergistic effect of rGO-Mn_3O_4 as well as Au composite, providing a large surface area and a lot of electroactive sites for DA to absorb and react. This shows that the modified electrode can be employed in the fabrication of a DA electrochemical sensor.

Selectivity, reproducibility and stability of the modified electrode

The selectivity of the modified electrode was assessed by adding different concentrations of common potential interfering species in the presence of 0.1 mmol·L^{-1} DA. The addition of 50-fold concentrations of NaCl, $CaCl_2$, glucose and acetaminophen, 10-fold concentrations of glutamic acid, lysine, uric acid, glycine, tryptophane, epinephrine, catecholamine, serotonin, resorcinol and hydroquinone caused no observable interference (signal change ±5%), indicating the excellent selectivity of the modified electrode.

The relative standard deviation (*RSD*) was 4.2% when the modified electrode was employed to determine 0.1 mmol·L^{-1} DA for five successive measurements. The *RSD* of the response currents to 0.1 mmol·L^{-1} DA was 3.2% for five modified electrodes fabricated in the same way, suggesting the excellent reproducibility of the modified electrode.

By storing the modified electrode in air at room temperature over four weeks, the stability of the modified electrode was investigated. The response current to 0.1 mmol·L^{-1} DA decayed by only 7.8% of its initial intensity (less than 10%), revealing the long-term stability of the modified electrode.

Real sample analysis

To verify the workability of the modified electrode, the DA injection solution was diluted 100 times with PB before analysis and without any other pretreatments. The reduction currents were recorded and the concentrations of DA were calculated from the calibration curve. The concentrations of DA in the injection solutions were found to be 52.5, 53.4, 52.4, 52.6, 52.7 and 52.7 mmol·L^{-1}, in accordance with the labeled value (52.7 mmol·L^{-1}). The recoveries vary from 99.2 to 102.4%. The results are shown in Table 2, demonstrating that the modified electrode is accurate and reliable for the detection of DA.

Conclusions

In this report, an electrochemical sensor based on GE sensitized with rGO-Mn_3O_4/ Nafion film supporting different sizes Au composite was fabricated. The modified electrode showed significantly improved selectivity and sensitivity, attributed to the modification of the composite. The sensor was applied to determine DA with good accuracy and recovery in real injection solution samples. The superior electrocatalytic performance enables the use of rGO-Mn_3O_4 and Au-based composite for the detection of other pharmaceutical and biological residues.

Acknowledgements The work was supported by the National Natural Science Foundation of China (No. 51672104 and No. 21675045), the Natural Science Foundation of Hunan Province (No. 2016JJ4071, No. 2017JJ2198) and the Foundation of Hunan Provincial Education Department (No.16B205 and No. 17C1148).

Compliance with ethical standards The author(s) declare that they have no competing interests.

References

1. Xu YQ, Hun X, Liu F, Wen XL, Luo XL (2015) Aptamer biosensor for dopamine based on a gold electrode modified with carbon nanoparticles and thionine labeled gold nanoparticles as probe. Microchim Acta 182:1797–1802. doi:10.1007/s00604-015-1509-5
2. Zhang QL, Feng JX, Wang AJ, Wei J, Lv ZY, Feng JJ (2015) A glassy carbon electrode modified with porous gold nanosheets for simultaneous determination of dopamine and acetaminophen. Microchim Acta 182:589–595. doi:10.1007/s00604-014-1363-x
3. Hsieh YS, Hong BD, Lee CL (2016) Non-enzymatic sensing of dopamine using a glassy carbon electrode modified with a nanocomposite consisting of palladium nanocubes supported on reduced graphene oxide in a nafion matrix. Microchim Acta 183:905–910. doi:10.1007/s00604-015-1668-4
4. Yan XY, Gu Y, Li C, Tang L, Zheng B, Li YR, Zhang ZQ, Yang M (2016) Synergetic catalysis based on the proline tailed metalloporphyrin with graphene sheet as efficient mimetic enzyme for ultrasensitive electrochemical detection of dopamine. Biosens Bioelectron 77:1032–1038. doi:10.1016/j.bios.2015.10.085
5. Sanghavi BJ, Wolfbeis OS, Hirsch T, Swami NS (2015) Nanomaterial-based electrochemical sensing of neurological drugs and neurotransmitters. Microchim Acta 182:1–41. doi:10.1007/s00604-014-1308-4
6. Wu BN, Miao CC, Yu LL, Wang ZY, Huang CS, Jia NQ (2014) Sensitive electrochemiluminescence sensor based on ordered mesoporous carbon composite film for dopamine. Sensors Actuators B Chem 195:22–27. doi:10.1016/j.snb.2014.01.012
7. Carrera V, Sabater E, Vilanova E, Sogorb MA (2007) A simple and rapid HPLC-MS method for the simultaneous determination of epinephrine, norepinephrine, dopamine and 5-hydroxytryptamine: application to the secretion of bovine chromaffin cell cultures. J Chromatogr B 847:88–94. doi:10.1016/j.jchromb.2006.09.032
8. Naccarato A, Gionfriddo E, Sindona G, Tagarelli A (2014) Development of a simple and rapid solid phase microextraction-gas chromatography-triple quadrupole mass spectrometry method for the analysis of dopamine, serotonin and norepinephrine in human urine. Anal Chim Acta 810:17–24. doi:10.1016/j.aca.2013.11.058
9. Wang HB, Zhang HD, Chen Y, Huang KJ, Liu YM (2015) A label-free and ultrasensitive fluorescent sensor for dopamine detection based on double-stranded DNA templated copper nanoparticles. Sensors Actuators B Chem 220:146–153. doi:10.1016/j.snb.2015.05.055
10. Lin FE, Gui C, Wen W, Bao T, Zhang XH, Wang SF (2016) Dopamine assay based on an aggregation-induced reversed inner filter effect of gold nanoparticles on the fluorescence of graphene

quantum dots. Talanta 158:292–298. doi:10.1016/j.talanta.2016.05.062

11. Hou SR, Zheng N, Feng HY, Li XJ, Yuan ZB (2008) Determination of dopamine in the presence of ascorbic acid using poly (3,5-dihydroxy benzoic acid) film modified electrode. Anal Biochem 381:179–184. doi:10.1016/j.ab.2008.03.055
12. Fernandes SC, Vieira IC, Peralta RA, Neves A (2010) Development of a biomimetic chitosan film-coated gold electrode for determination of dopamine in the presence of ascorbic acid and uric acid. Electrochim Acta 55:7152–7157. doi:10.1016/j.electacta.2010.06.062
13. Huang Y, Cheng CM, Tian XQ, Zheng BZ, Li Y, Yuan HY, Xiao D, Choi MMF (2013) Low-potential amperometric detection of dopamine based on MnO_2 nanowires/chitosan modified gold electrode. Electrochim Acta 89:832–839. doi:10.1016/j.electacta.2012.11.071
14. Sajid M, Nazal MK, Mansha M, Alsharaa A, Jillani SMJ, Basheer C (2016) Chemically modified electrodes for electrochemical detection of dopamine in the presence of uric acid and ascorbic acid: a review. TrAC Trends Anal Chem 76:15–29. doi:10.1016/j.trac.2015.09.006
15. Li Y, Lin HC, Peng H, Qi RJ, Luo CH (2016) A glassy carbon electrode modified with MoS_2 nanosheets and poly(3,4-ethylenedioxythiophene) for simultaneous electrochemical detection of ascorbic acid, dopamine and uric acid. Microchim Acta 183:2517–2523. doi:10.1007/s00604-016-1897-1
16. Jin JY, Mei H, Wu HM, Wang SF, Xia QH, Ding Y (2016) Selective detection of dopamine based on Cu_2O@Pt core-shell nanoparticles modified electrode in the presence of ascorbic acid and uric acid. J Alloys Compd 689:174–181. doi:10.1016/j.jallcom.2016.07.322
17. Numan A, Shahid MM, Omar FS, Ramesh K, Ramesh S (2017) Facile fabrication of cobalt oxide nanograin-decorated reduced graphene oxide composite as ultrasensitive platform for dopamine detection. Sensors Actuators B Chem 238:1043–1051. doi:10.1016/j.snb.2016.07.111
18. Ejaz A, Joo Y, Jeon SW (2017) Fabrication of 1,4-bis(aminomethyl)benzene and cobalt hydroxide @graphene oxide for selective detection of dopamine in the presence of ascorbic acid and serotonin. Sensors Actuators B Chem 240:297–307. doi:10.1016/j.snb.2016.08.171
19. Sivasubramanian R, Biji P (2016) Preparation of copper (I) oxide nanohexagon decorated reduced graphene oxide nanocomposite and its application in electrochemical sensing of dopamine. Mater Sci Eng B 210:10–18. doi:10.1016/j.mseb.2016.04.018
20. Khudaish EA, Al-Nofli F, Rather JA, Al-Hinaai M, Laxman K, Kyaw HH, Al-Harthy S (2016) Sensitive and selective dopamine sensor based on novel conjugated polymer decorated with gold nanoparticles. J Electroanal Chem 761:80–88. doi:10.1016/j.jelechem.2015.12.011
21. Jia LP, Zhou YX, Jiang YM, Zhang AH, Li X, Wang CM (2016) A novel dopamine sensor based on Mo doped reduced graphene oxide/polyimide composite membrane. J Alloys Compd 685:167–174. doi:10.1016/j.jallcom.2016.05.239
22. Zhang DD, Li LZ, Ma WN, Chen X, Zhang YM (2017) Electrodeposited reduced graphene oxide incorporating polymerization of L-lysine on electrode surface and its application in simultaneous electrochemical determination of ascorbic acid, dopamine and uric acid. Mater Sci Eng C 70:241–249. doi:10.1016/j.msec.2016.08.078
23. Vilian ATE, An SY, Choe SR, Kwak CH, Huh YS, Lee JH, Han YK (2016) Fabrication of 3D honeycomb-like porous polyurethane-functionalized reduced graphene oxide for detection of dopamine. Biosens Bioelectron 86:122–128. doi:10.1016/j.bios.2016.06.022
24. Li XJ, Song ZW, Zhao Y, Wang Y, Zhao XC, Liang MH, Chu WG, Jiang P, Liu Y (2016) Vertically porous nickel thin film supported Mn_3O_4 for enhanced energy storage performance. J Colloid Interface Sci 483:17–25. doi:10.1016/j.jcis.2016.08.006
25. Xu JS, Fan XM, Xia Q, Shao ZM, Pei B, Yang ZH, Chen ZX, Zhang WX (2016) A highly atom-efficient strategy to synthesize reduced graphene oxide-Mn_3O_4 nanoparticles composites for supercapacitors. J Alloys Compd 685:949–956. doi:10.1016/j.jallcom.2016.06.247
26. Zhen MM, Zhang Z, Ren QT, Liu L (2016) Room-temperature synthesis of ultrathin Mn_3O_4 nanosheets as anode materials for lithium-ion batteries. Mater Lett 177:21–24. doi:10.1016/j.matlet.2016.04.156
27. Singh N, Ali MA, Suresh K, Agrawal VV, Rai P, Sharma A, Malhotra BD, John R (2016) In-situ electrosynthesized nanostructured Mn_3O_4-polyaniline nanofibers-biointerface for endocrine disrupting chemical detection. Sensors Actuators B Chem 236:781–793. doi:10.1016/j.snb.2016.06.050
28. Yusoff N, Pandikumar A, Ramaraj R, Lim HN, Huang NM (2015) Gold nanoparticle based optical and electrochemical sensing of dopamine. Microchim Acta 182:2091–2114. doi:10.1007/s00604-015-1609-2
29. Khudaish EA, Rather JA (2016) Electrochemical studies of dopamine under stagnant and convective conditions at a sensor based on gold nanoparticles hosted in poly(triaminopyrimidine). J Electroanal Chem 776:206–212. doi:10.1016/j.jelechem.2016.06.041
30. Li SJ, Deng DH, Shi Q, Liu SR (2012) Electrochemical synthesis of a graphene sheet and gold nanoparticle-based nanocomposite, and its application to amperometric sensing of dopamine. Microchim Acta 177:325–331. doi:10.1007/s00604-012-0782-9
31. Salimi A, Abdi K, Khayatian GR (2004) Amperometric detection of dopamine in the presence of ascorbic acid using a nafion coated glassy carbon electrode modified with catechin hydrate as a natural antioxidant. Microchim Acta 144:161–169. doi:10.1007/s00604-003-0048-7
32. Yang X, Xiao FB, Lin HW, Wu F, Chen DZ, Wu ZY (2013) A novel H_2O_2 biosensor based on Fe_3O_4-au magnetic nanoparticles coated horseradish peroxidase and graphene sheets-nafion film modified screen-printed carbon electrode. Electrochim Acta 109:750–755. doi:10.1016/j.electacta.2013.08.011
33. Yang X, Ouyang YJ, Wu F, Hu YJ, Ji Y, Wu ZY (2017) Size controllable preparation of gold nanoparticles loading on graphene sheets@cerium oxide nanocomposites modified gold electrode for nonenzymatic hydrogen peroxide detection. Sensors Actuators B Chem 238:40–47. doi:10.1016/j.snb.2016.07.016
34. Cao X, Cai XL, Wang N (2011) Selective sensing of dopamine at MnOOH nanobelt modified electrode. Sensors Actuators B Chem 160:771–776. doi:10.1016/j.snb.2011.08.061
35. Abdelwahab AA, Lee HM, Shim YB (2009) Selective determination of dopamine with a cibacron blue/poly-1,5-diaminonaphthalene composite film. Anal Chim Acta 650:247–253. doi:10.1016/j.aca.2009.07.054
36. Adekunle AS, Agboola BO, Pillay J, Ozoemena KI (2010) Electrocatalytic detection of dopamine at single-walled carbon nanotubes-iron (III) oxide nanoparticles platform. Sensors Actuators B Chem 148:93–102. doi:10.1016/j.snb.2010.03.088
37. Kumar MK, Prataap RV, Mohan S, Jha SK (2016) Preparation of electro-reduced graphene oxide supported walnut shape nickel nanostructures, and their application to selective detection of dopamine. Microchim Acta 183:1759–1768. doi:10.1007/s00604-016-1806-7
38. Rao D, Zhang X, Sheng Q, Zheng J (2016) Highly improved sensing of dopamine by using glassy carbon electrode modified with MnO_2, graphene oxide, carbon nanotubes and gold nanoparticles. Microchim Acta 183:2597–2604. doi:10.1007/s00604-016-1902-8